Electrochemical Oxidation of Wastewater Contaminated with Astrazon Red Violet 3RN Dye on $Ti/IrO_2/RuO_2$: Evaluation of Process Parameters, Kinetics, and Energy Consumption

Sözüdoğru, Onur*+

Department of Emergency Aid and Disaster Management, Faculty of Applied Science, Ataturk University, Erzurum, TURKEY

ABSTRACT: *The performance of the electrochemical oxidation of wastewater contaminated with Astrazon Red Violet 3RN Dye on $Ti/IrO_2/RuO_2$ was evaluated under a range of significant process variables: support electrolyte type and concentration, initial dye concentration, pH, current density, and temperature. ARV-3RN dye removal efficiency was over 90% at the high concentrations of NaCl (≥ 5.0 mM) and lower pH values (3.0 ≤ pH≤ ~7.5). At the same time, the temperature increases promoted faster degradation and less energy consumption except at 10°C temperature. While the increase in the initial dye concentration had a negative effect on the removal efficiency (from 99.84% to 65.02%), energy consumption increased from 2.5 kW-h/m^3 to 3.25 kW-h/m^3. Although the change in applied current density did not cause a significant difference in the removal efficiency (from 99.34% to 92.79%), it caused the energy consumption to increase from 3.10 kW-h/m^3 to 25.767 kW-h/m^3. Electrooxidation kinetics were evaluated using Pseudo-zero-order, Pseudo-first-order, and pseudo-second-order models. Kinetic data fitted best Pseudo-first-order model. The activation energy (E_a) of the* EAOP *process calculated using the Arrhenius equation is 13.707 kJ/mol. Thermodynamic parameters $\Delta H°$, $\Delta S°$, and $\Delta G°$ evaluated by Eyring's equation calculated 11.196 kJ/mol, -0.1244 kJ/mol, and 47.662 for 293 K, respectively.*

KEYWORDS: *Electrochemical Oxidation, Decolorization, Corrosion treatment, Operating parameters, Energy consumption, Kinetics, Thermodynamics.*

INTRODUCTION

Freshwater is one of the most vital things for human life. However, as urbanization, population, and industrialization increased rapidly worldwide, people began contaminating natural water sources with various home and industrial effluents [1]. Heavy metals, dyes, medicines, polyaromatic hydrocarbons (PAHs), polychlorinated biphenyls, acidic and basic effluents, and pesticides are just a few dangerous chemical compounds found in complex wastewater matrices [2–5]. Synthetic dyes are a significant class of corrosive organic compounds frequently found in wastewater as environmental pollutants due to their extensive industrial use. [6]. A large volume of dyes is widely used by several sectors, including the textile (60%), leather tannery (60%),

* *To whom correspondence should be addressed.*
+E-mail: cm.onursozudogru@gmail.com & onur.sozudogru@atauni.edu.tr
1021-9986/2023/11/3640-3658 19/$/6.09

paper (10%), and packaging industries (10%), and they are a significant source of pollution [7–9]. Even though residual dyes are only present in measurable amounts in wastewater, they must be eliminated before the wastewater is disposed of because the discharge of this colored wastewater into natural water bodies affects biological processes in the aquatic environment, restricts oxygen diffusion, blocks light penetration and causes an undesirable appearance [10–14]. Also, azo dyes pose a severe threat to the aquatic system and human health because of their adverse side effects, which include mutagenicity, skin irritation, allergy, and carcinogenicity [6, 15, 16].

Some synthetic organic dyes are slow to degrade or non-biodegradable, which makes wastewater treatment in Conventional Wastewater Treatment Plants (CWTP) more challenging. Due to the dye's sizeable molecular weight, aromatic rings, reactive functional groups, and great biochemical stability, conventional treatment plants typically cannot effectively remove dye effluents [17, 18]. As a result of their resistance to common treatments such as coagulation-flocculation, biological oxidation, adsorption, ion exchange, and chemical oxidation, the great majority of dyes are called persistent organic pollutants [19, 20]. For these reasons, there has been growing interest in the use of advanced technology such as ozonation, Fenton, photo-Fenton, electro-Fenton, photocatalysis, radiation, sonolysis, and electrochemical oxidation (electrooxidation (EAOP)) which has been proven to be promising and attractive technology in the effective degradation of recalcitrant organic compounds like dyes in wastewater [21, 22].

Recent research on the removal of organic dyes from wastewater promotes their removal by electrochemical methods [23]. EAOP is a highly effective method that can break down even the most biorefractory organic pollutants in wastewater [24, 25]. The ability of EAOP to transform hazardous compounds into non-hazardous or low-toxicity chemicals draws attention [26–28]. Compared to other advanced oxidation methods, it offers several advantages, including simplicity, selectivity, flexibility, high energy efficiency, without chemical additions, without producing sludge, automation amenability, the safety of operation under mild conditions, environmental friendliness, and financial viability [29–31]. Hydroxyl radicals ($^{\bullet}OH$) ($E° = 2.8$ V/SHE) generated electrolytically are used by EAOPs to mineralize organic contaminants [32, 33]. EAOPs may be categorized into two groups based on the generation of $^{\bullet}OH$ in the electrolytic system: direct and mediated EAOPs [34, 35]. The MO_X ($^{\bullet}OH$) principal process is that ($^{\bullet}OH$) hydroxyl radicals are generated on the metal oxide MO_X anode surface by direct oxidation of water Eq. (1) [36]. The Process is heterogeneous, and the anode surface absorbs the generated hydroxyl radicals. $MO_X(^{\bullet}OH)$ transform into MO_{X+1} or evolve to oxygen Eq. (2) and Eq. (3). Chemisorbed oxygen (MO_{X+1}) can be selectively converted refractory organics (RH) to biodegradable by-products (RHO) and produces oxygen (O_2) as in Eq. (4). The generated $^{\bullet}OH$ radical can be physisorbed oxidant ($MO_X(^{\bullet}OH)$) onto the anode surface and $MO_X(^{\bullet}OH)$ causes the complete mineralization of the organic pollutants (RH) into H_2O, CO_2, and inorganic ions Eq. (5) and Eq. (6) [37–40].

$$MO_x + H_20 \rightarrow MO_x(^{\bullet}OH) + H^+ + e^- \quad (1)$$

$$MO_x(^{\bullet}OH) \rightarrow MO_{x+1} + H^+ + e^- \quad (2)$$

$$MO_{x+1} \rightarrow MO_x + 0.5O_2 \quad (3)$$

$$MO_{x+1} + RH \rightarrow MO_x + RHO + H_20 + H_+ + e^- \quad (4)$$

$$MO_x(^{\bullet}OH) + RH \rightarrow MO_x + mH_2O + nCO_2 + H^+ + e^- \quad (5)$$

$$MO_x(^{\bullet}OH) \rightarrow MO_x + H^+ + e^- + 0.5O_2 \quad (6)$$

One of the key points in explaining the high efficiencies achieved by EAOPs in removing organic pollutants is to understand the role played by oxidation processes that occur indirectly during the general oxidation in the treatment. Mediated oxidation can be defined as the oxidation of pollutants with strong oxidizers such as $^{\bullet}OH$, $^{\bullet}CI$, $^{\bullet}SO4^-$, hydrogen peroxide, ozone, peroxodisulfate ($S_2O_8^{2-}$), peroxodiphosphate ($P_2O_8^{4-}$), and peroxodicarbonate ($C_2O_6^{2-}$) generated in wastewater depending on the electrolyte composition and electrode materials [41–43].

This study aimed to investigate an efficient EAOP system using $Ti/IrO_2/RuO_2$ anode for ARV-3RN dye removal. Additionally, efficient and cost-effective process conditions were determined by examining the impact of process variables on energy consumption and removal efficiency. Therefore, the initial concentration of ARV-3RN dye (50-1000 mg/L), current density (0.44-1.79 mA/cm^2), initial pH (3.0-11.0), temperature (10-55 °C), supporting electrolyte type (NaCl, KCl, $NaNO_3$, and Na_2SO_4) and concentration (2.5-10 mM NaCl) were chosen as the system variables for investigation in this study, as suggested by prior research showing that the electrochemical

Table 1: Properties and molecular structure of the ARV-3RN dye

Properties	Chemical structure
Molecular formula: $C_{23}H_{29}ClN_2$	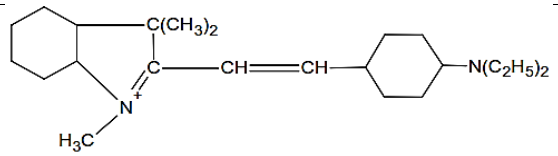
Molecular weight: 368.943 g/mol	
λ_{max}/nm: 547	
CAS number: 6359-45-1	

degradation of organic pollutants primarily depends on specific system variables.

EXPERIMENTAL SECTION

Material

All analytical grade chemicals that include ARV-3RN dye, nitric acid (HNO_3) (68%), sodium hydroxide (NaOH) (≥ 98%), Sodium chloride (NaCl) (≥ 99%), Potassium chloride (KCl) (≥ 99%), Sodium sulfate (Na_2SO_4) (≥ 99%), and Sodium Nitrate ($NaNO_3$) (≥ 99%) used throughout experimental studies were purchased from Sigma-Aldrich. The properties and molecular structure of the ARV-3RN dye are illustrated in Table 1. ARV-3RN dye stock solution was prepared as 1000 mg/L with 1 L of distilled water.

Experimental setup and analytical procedures

The effects of variables, including pH, electrolyte type and concentration, current density, temperature, and initial dye concentration on the elimination of ARV-3RN dye by EAOP were worked in batch mode. All experiments were conducted in a jacketed glass reactor in which 70x100x2 mm dimension electrodes were positioned parallelly. Also, $Ti/IrO_2/RuO_2$ mesh plates as anode and stainless steel as cathode were used in the reactor. 5 anode and 5 cathode mesh plates were used for a total surface area of 2240 cm^2. The electrodes were placed parallel to the reactor with 0.5 cm spaces to prevent ohmic losses. 1.2L of synthetic ARV-3RN dye solution for each run was filled into the reactor. The required electrical current was supplied by a digitally controlled direct current supply (KXN-3050D DC-Power Supply). A magnetic stirrer (Heidolph MR Hei-End) was used to mix the dye solution homogeneously in the reactor. The solution's initial pH was adjusted with analytical grade 0.1 M HNO_3 (68%) and 0.1 M NaOH (≥ 98%); pH was checked during the experiment, but no pH adjustments were done. A cooling heating circulator controlled the reactor temperature. The sample temperature, conductivity, and pH were continuously measured using the WTW multi-340i multimeter. Color measurement of the samples taken at regular intervals up to 60 min of reaction time was made with a spectrophotometer (Spekol-1100-UV-Vis spectrophotometer) at a wavelength of 547 nm. The electrochemical cell was properly washed after each batch experiment to prevent the electrode surface's passivation. The setup of a lab-scale EAOP system is shown in Fig. 1.

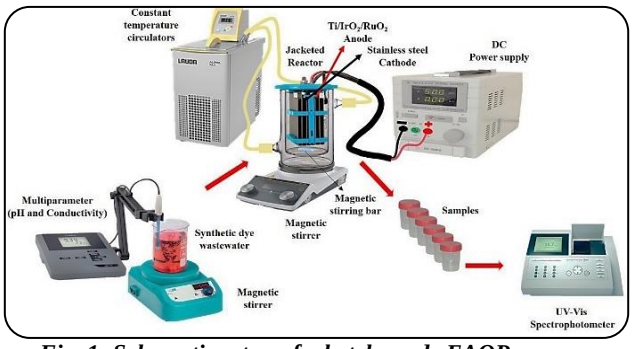

Fig. 1: Schematic setup of a batch-mode EAOP process.

Table 2: Equations of kinetic models

Kinetic Model	Mathematical equations	Pilots	Equations
Pseudo-zero-order kinetic	$C_t = C_0 - k_0 t$	C_0-C_t versus t	(8)
Pseudo-first-order kinetic	$\ln(\frac{C_0}{C_t}) = k_1 t$	ln (C_t/C_0) versus t	(9)
Pseudo-second-order kinetic	$\frac{1}{C_t} = \frac{1}{C_0} + k_2 t$	t/C_t versus t	(10)

The dye removal efficiency obtained by electrochemical oxidation was determined utilizing Eq. (7):

$$Removal efficiency(\%) = (1 - \frac{C_e}{C_0}) \times 100 \qquad (7)$$

Where C_0 and C_e are expressed as the initial dye concentration (mg/L) and final dye concentration (mg/L), respectively.

Pseudo-zero-order kinetics, pseudo-first-order kinetics and pseudo-second-order kinetics were used to calculate the electrochemical oxidation kinetics of ARV-3RN dye with the kinetics shown in Table 2. Where k_0, k_1, and k_2 represent pseudo-zero-order (mg/L.min) and pseudo-first-order (1/min) and pseudo-second-order (L/mg.min) rate constant, respectively. C_0 is the initial concentration of ARV-3RN

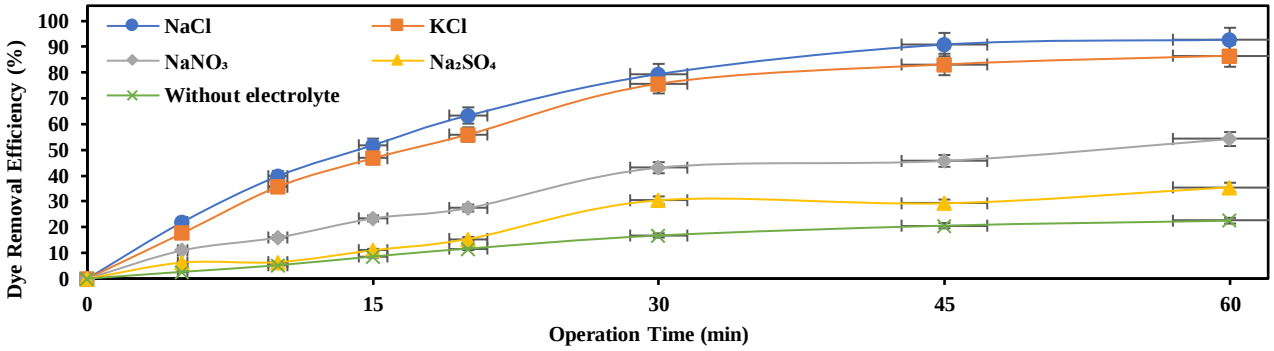

Fig. 2: Effect of type of support electrolyte on ARV-3RN dye removal efficiency

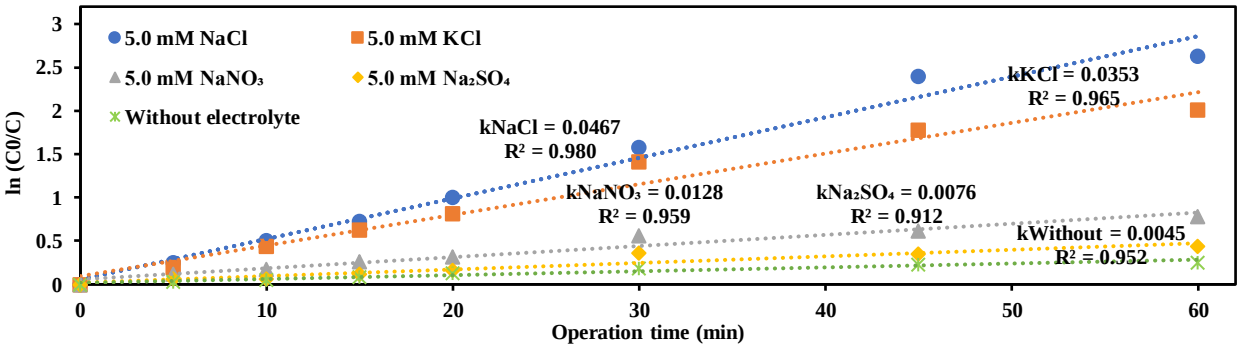

Fig. 3: Pseudo-first-order kinetics fitting for support electrolyte type

dye (mg/L), C_t is the concentration of ARV-3RN dye at t time (mg/L), and t is the reaction time (min). The kinetic parameters were obtained by fitting the experimental data with linear regression.

The energy consumption is defined as the amount of energy consumed per unit m^3 of dye degraded and expressed in kW-h/m^3 of dye removed and was calculated based on the following Eq. (11):

$$Energy consumption; EC(kW - h/m^3 wastewater) = \frac{V \times I \times t}{v} \quad (11)$$

Where V (volt) is the average cell voltage, I (ampere) is current, t is the electrolysis time (min), and v (m^3) is the total ARV-3RN dye volume.

RESULTS AND DISCUSSION

Effect of supporting electrolyte type on removal efficiency and rate constant

Electrooxidation degradation can only proceed in electrically conductive solutions. The decolorization efficiency of the EAOP Process is determined by the supporting electrolyte type and concentration added to the solution to provide electrical conductivity. The most effective several salts (KCl, NaCl, Na_2SO_4, and $NaNO_3$) were investigated as supporting electrolytes in the EAOP process. At a constant current density of 0.44 mA/cm^2, 5.0 mM support electrolytes were added to 250 mg/L dye solution at initial pH (≈7.5), and the efficiency of ARV-3RN dye removal was determined over a reaction time of 60 min. Fig. 2. According to the findings, electrolytes added to the solution increased the dye removal efficiency at the end of the electrolysis time. ARV-3RN dye removal efficiencies for the runs NaCl, KCl, Na_2SO_4, and $NaNO_3$ were 92.79%, 86.60%, 54.20%, and 35.45%, respectively. To analyze the oxidation kinetic behaviour of the electrochemical oxidation of ARV-3RN, oxidation kinetic models' equations were given in Table 2. Fig. 3. showed a good linear correlation between ln(C_0/C) and electrolysis time (t) ($R^2 > 0.98$) for 5.0 mM NaCl support electrolyte. According to the supporting electrolyte type, k values can be ordered as NaCl> KCl> $NaNO_3$> Na_2SO_4. The active chlorine species that causes indirect oxidation is the reason for the high reaction rate. The larger ionization capacity of the NaCl electrolyte than the KCl electrolyte can explain why it is more successful at removing dye [44, 45]. NaCl is also easy to obtain and has relatively high solubility [39].

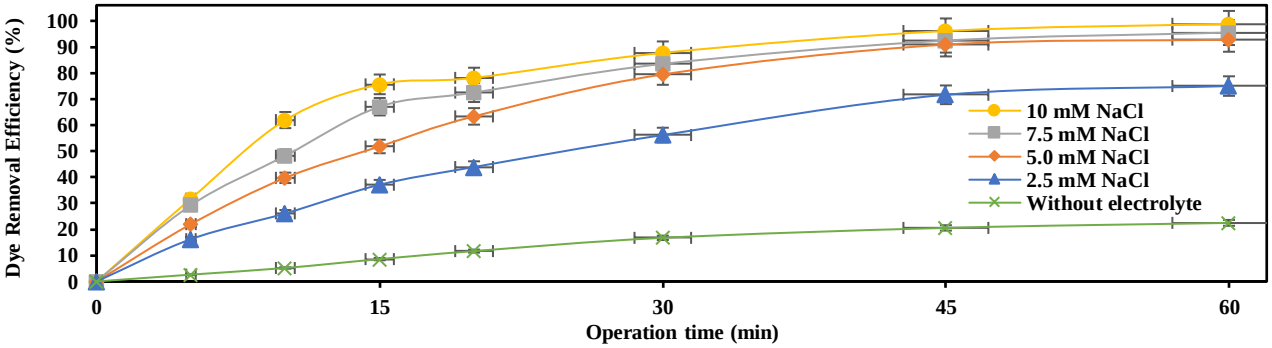

Fig. 4: Effect of support electrolyte concentration on ARV-3RN dye removal efficiency

ARV-3RN dye removal efficiency increased significantly with all salts used in the studies.

Compared to Na_2SO_4 and $NaNO_3$, NaCl and KCl electrolytes are much more effective in removing ARV-3RN dye. The production of different oxidant types associated with the type of salt in this medium may be involved. Chlorine was added to promote the electrochemical generation of active chlorine species, such as the powerful oxidants Cl_2, HOCl, and OCl^- dependent on the current density and pH of the solution [46]. $NaNO_3$, an inert electrolyte, has no ions in its structure that may function as an indirect oxidant [47, 48]. Also, $NaNO_3$ and polymeric species in the wastewater block the electrode surfaces and deactivate the active sites on the electrode surfaces. Thus, The efficiency decrease of electrochemical oxidation is due to the contamination/passivation of the working electrode surface [49–51]. The Na_2SO_4 electrolyte produces $^{\bullet}SO_4^-$ and $S_2O_8^-$, which are weak oxidants that indirectly degrade the dye, but over time SO_4^{-2} scavenges the $^{\bullet}OH$ (Eqs. (12), (13), (14), and (15)) [26, 52, 53]. Similar results are available in studies investigating the effect of the supporting electrolyte type on electrochemical reactions [53, 54].

$$2H_2O \rightarrow 2\ {}^{\bullet}OH + 2H^+ + 2e^- \quad (12)$$

$$2SO_4^{-2} \rightarrow S_2O_8^{-2} + 2e^- \quad (13)$$

$$SO_4^{-2} + {}^{\bullet}OH \rightarrow SO_4^{-\bullet} + OH^- \quad (14)$$

$$SO_4^{-\bullet} + SO_4^{-\bullet} \rightarrow S_2O_8^{-2} \quad (15)$$

Effect of support electrolyte concentration on removal efficiency and rate constant

Sodium chloride (NaCl) was chosen as a supporting electrolyte in this study because of its low cost, high solubility, and the production of strong oxidizing active chlorine species. The effect of support electrolyte concentration on the ARV-3RN dye removal was carried out to examined at a constant current density of 0.45 mA/cm^2, initial pH (≈7.5), the temperature of 20 °C, the synthetic ARV-3RN dye concentration of 250 mg/L, a certain amount of NaCl (2.5 mM, 5.0 mM, 7.5 mM, and 10 mM), and reaction time of 60 min. The efficiency of ARV-3RN dye removal for the runs of 2.5 mM NaCl, 5.0 mM NaCl, 7.5 mM NaCl, and 10 mM NaCl was found to be 74.98%, 92.79%, 95.50%, and 98.87%, respectively. The data obtained are given in Fig. 4. According to the calculations made according to the kinetic equations given in Table 2, it is demonstrated in Fig. 5. to be a linear correlation between $\ln(C_0/C)$ and operation time (t) for all NaCl concentrations. It can be concluded that the k values increased as the concentration of the supporting electrolyte increased. As the support electrolyte concentration increased from 2.5 mM NaCl to 10 mM NaCl, the *k* value ranged from 0.0239 to 0,0718 1/min.

The production of more active chlorine species such as Cl_2, HClO, and ClO^- (Eqs. (16), (23), and (24)), which quickly oxidize the ARV-3RN dye, is connected to the increase in the reaction rate with increasing support electrolyte concentration. The addition of NaCl, which enhanced the solution's conductivity, not only decreased energy consumption but also contributed to powerful oxidizing agents and decreased the electrodes' passivity by eliminating the passive oxide layer from their surface due to its catalytic effect [55, 56]. The solution's electrical conductivity significantly impacts the rate of decolorization. Conductivity affects a higher degradation ratio, faster electron transport, and energy savings [57]. NaCl controls the formation of reactive chlorine species like Cl_2, HClO, and ClO^- [24, 39, 58]. The indirect oxidation *via* the chlorine/hypochlorite generated during the electrolysis

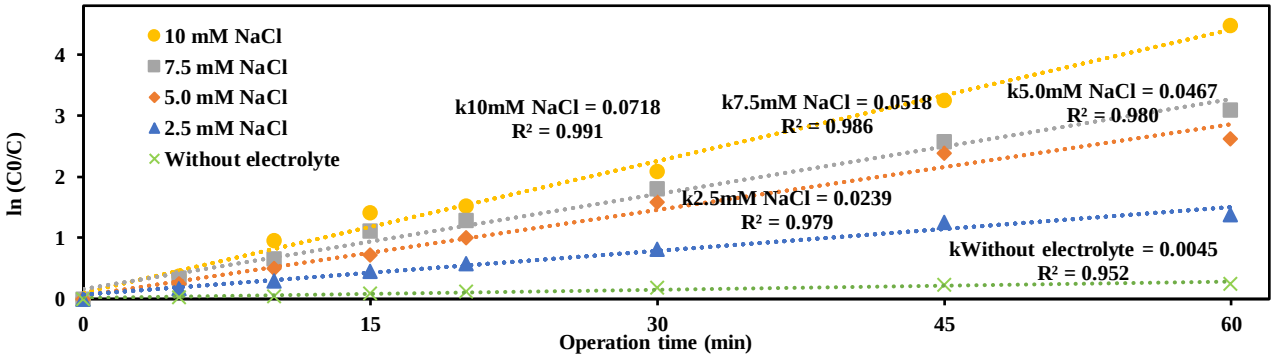

Fig. 5: Pseudo-first-order kinetics fitting for support electrolyte concentration

in the NaCl medium might be primarily responsible for the elimination of the synthetic dye in the electrochemical oxidation [59–61]. More electro-active chlorine oxidizing species were formed at higher NaCl concentrations, increasing the percentage of ARV-3RN dye removed.

Anodic reactions

$$2Cl^- \rightarrow Cl_2 + 2e^- \quad (16)$$

$$6HOCl + 3H_2O \rightarrow 2ClO_3^- + 4Cl^- + 12H^+ + 1.5O_2 + 6e^- \quad (17)$$

$$2H_2O \rightarrow O_2 + 4H^+ + 6e^- \quad (18)$$

Cathodic reactions

$$2H_2O + 2e^- \rightarrow 2OH^- + H_2 \quad (19)$$

$$OCI^- + 2H_2O + 2e^- \rightarrow Cl^- + 2OH^- \quad (20)$$

$$6ClO^- + 3H_2O \rightarrow 2ClO_3^- + 4CI^- + 6H^+ + \frac{3}{2}O_2 + 6e^- \quad (21)$$

$$ClO_3^- + H_2O \rightarrow ClO_4^- + 2H + 2e^- \quad (22)$$

Solution reactions

$$Cl_2 + H_2O \rightarrow HOCl + H^+ + Cl^- \quad (23)$$

$$HOCl \Leftrightarrow H^+ + OCl^- \quad (24)$$

Malpass et al. [62] and *Miwa et al*. [63] also offered evidence for the crucial role of NaCl in decolorization. *Viana et al*. [64] stated that in the removal of reactive Black 5 dye by electrooxidation using Ti/$(RuO_2)_{0.8}$-$(Sb_2O_3)_{0.2}$ electrode, the dye removal improved from 13.79% to 80.45% by increasing NaCl from 0.03 M to 0.1 M. Another study that used platinum-coated titanium electrodes to remove Drimaren Orange HF 2GL reported that the removal efficiency improved as the NaCl concentration increased [44].

Effect of initial pH on removal efficiency and rate constant

Numerous researchers have investigated how the solution's initial pH affects degradation processes, and the results indicate that this initial pH is essential for the electrocatalytic breakdown of organic contaminants. Because it may change the morphology of species that have degraded and the surface charge of the catalyst throughout the wastewater treatment process, the pH of the wastewater is a frequent factor impacting the removal of organic contaminants ((46,47,48)). To investigate the effects of the initial pH on ARV-3RN dye removal, the initial pH was set to five levels 3.0, 5.0, natural (≈7.5), 9.0, and 11.0, with other factors unchanged (0.45 mA/cm^2 current density, 5.0 mM NaCl support electrolyte, 20 °C temperature, 250 mg/L dye concentration and 60 min reaction time). As shown in Fig. 6. at 60 min, the dye removal efficiencies were 99.67%, 98.14%, and 92.79% at pH 3.0, 5.0, and natural (≈7.5), respectively. At pH above the natural pH (9.0 and 11.0), the dye removal efficiency is below 70%. The removal efficiencies for pH 9.0 and 11.0 were 69.00% and 62.97%, respectively. Changing the initial pH affected decolorization efficiency

Fig. 7. shows a better linear correlation (>98) between the removal efficiency and electrolysis time in the acidic and neutral media compared to the basic media. The results showed the following decolorization reaction rate order: $k_{pH:3.0} > k_{pH:5.0} > k_{pH:\approx7.5} > k_{pH:9.0} > k_{pH:11.0}$. Because of the production of powerful oxidizing agents such as Cl_2, HClO, and ClO^- during the electrolysis time, the addition of support like chloride can accelerate the breakdown

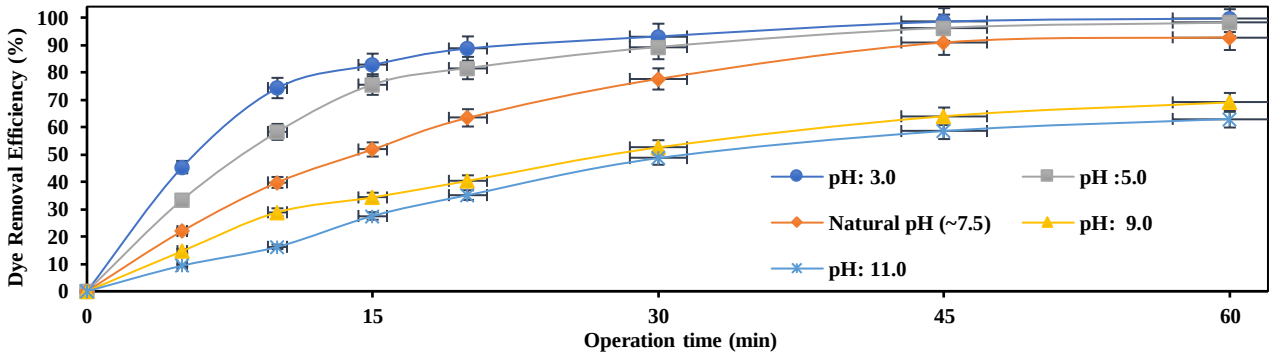

Fig. 6: Effect of initial pH on removal of ARV-3RN dye

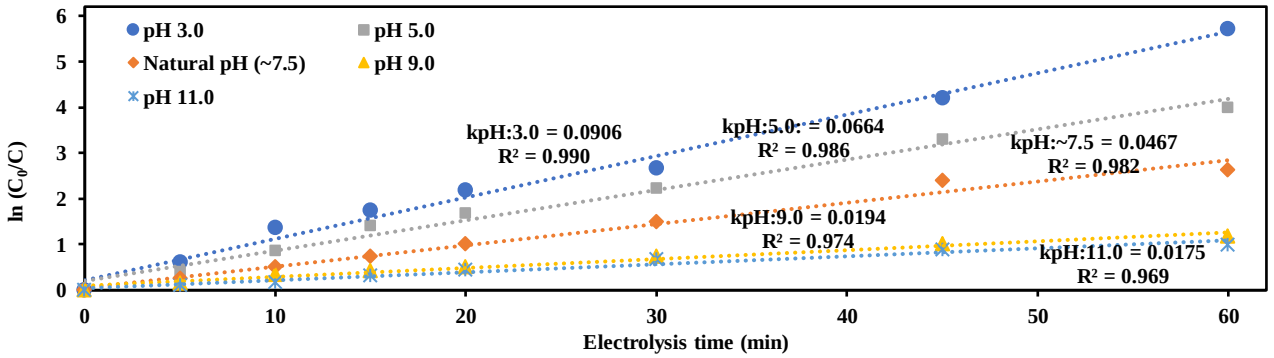

Fig. 7: Pseudo-first-order kinetics fitting for initial pH

of organic contaminants in wastewater. These species can convert organic pollutant molecules into non-polluting species, such as CO_2 and H_2O, or less harmful products [65]. The dominating reactive chlorine species depend on the pH of the solution (pH ≈3.0 for Cl_2, 3.0< pH <8.0 for HCIO, and pH> 8.0 for ClO^- (Eqs. (16), (23), and (24)) [66] and have standard potentials (E°) of 1.36 V, 1.49 V, and 0.89 V for $Cl_{2(aq)}$, HClO, and ClO^-, respectively [67]. Also, some available types of chlorine, such as HCIO and ClO^- in very alkaline conditions, would be transformed into ClO_3^- or ClO_4^- ions (Eqs. (17), (21), and (22)), which have weak oxidation capacity for organic removal, and these agents are responsible for the EAOP process poor performance at basic pHs [59, 68, 69].

The effectiveness of the EAOP process depends on variations in pH during the operation time as well as on the initial pH. As seen in Fig. 8. it reveals that the pH changes from intermediates during the degradation of the dye.

Current density on removal efficiency and rate constant

The impact of constant current density on the decolorization was investigated at 0.44 mA/cm^2, 0.89 mA/cm^2, 1.33 mA/cm^2, and 1.78 mA/cm^2 current densities at initial pH (≈7.5), initial dye concentration of 250 mg/L, support electrolyte of 5.0 mM NaCl, the temperature of 20 °C, and electrolysis time of 60 min. The results for 0.44 mA/cm^2, 0.89 mA/cm^2, 1.33 mA/cm^2, and 1.78 mA/cm^2 current densities on ARV-3RN dye removal for each applied current density are; 92.79%, 94.33%, 96.54, and 99.34, respectively.

As shown in Fig. 9. Current density significantly impacts the electrochemical elimination of ARV-3RN dye since it provides the force that drives charge migration. After 60 min of electrolysis, the ARV-3RN dye removal increased from 92.79% to 99.34%, and the rate constant from 0.0467 1/min to 0.0838 1/min when the current density increased from 0.44 to 1.78 mA/cm^2 (Fig. 10.). For this situation, it can be stated that the increase in current density considerably speeds up the elimination process of contaminants due to the increased rate of production of oxidants such as $^{\bullet}OH$, Cl_2, HClO, and ClO^- at higher current densities [59, 70, 71]. The rate of the electro-degradation reaction is controlled by current density, which is one of the critical variables in the EAOP process [72]. Applied current

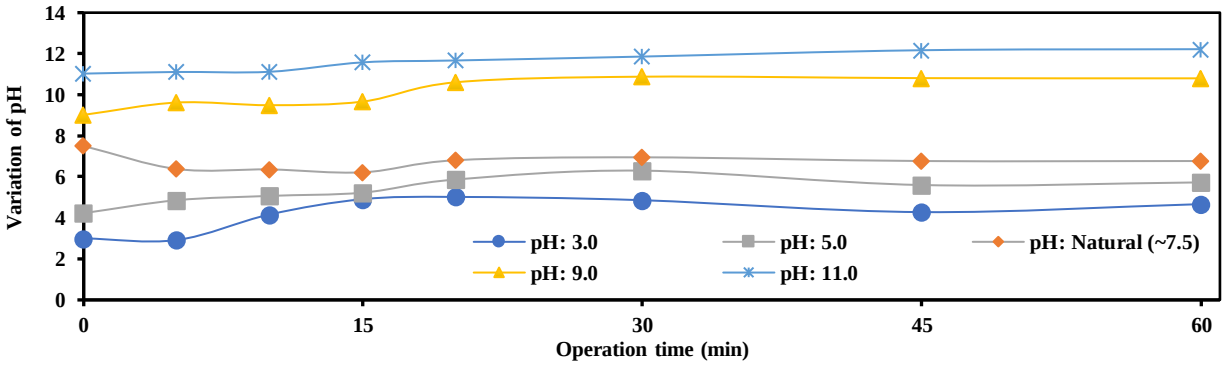

Fig. 8: The variation of pH values during the operation time

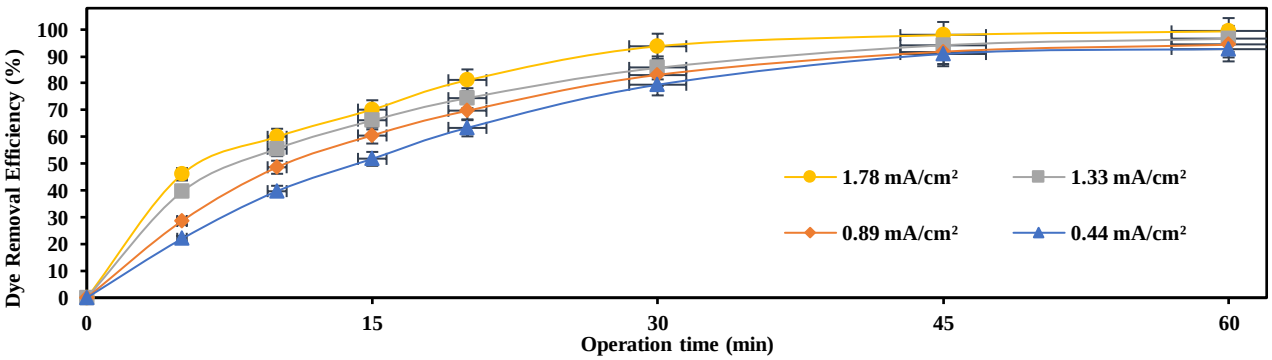

Fig. 9: Effect of current density on color removal efficiency

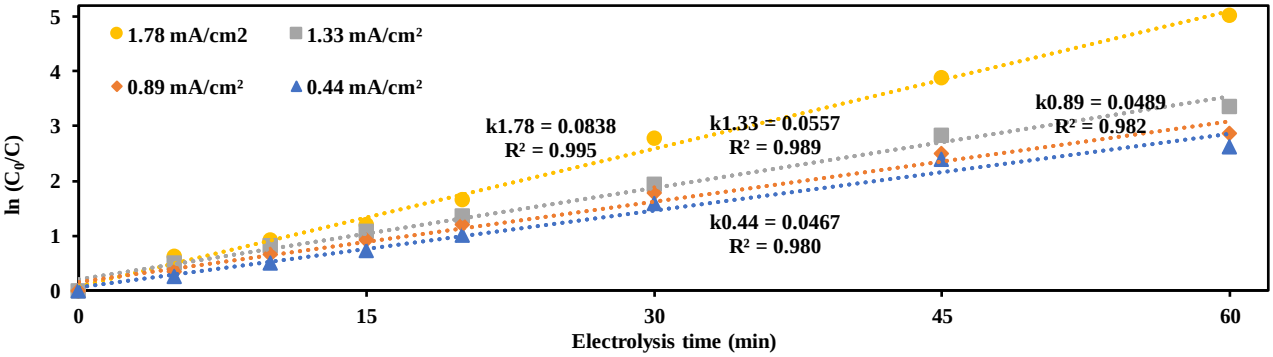

Fig. 10: Pseudo-first-order kinetics fitting for current density

density regulates the electron transfer, and the quantity of radical •OH generated on the electrode surface would directly affect how quickly organic pollutants were removed. [73]. However, it is known that higher current densities cause undesired side reactions, such as parasitic reactions, which cause the depletion of ClO^- (Eqs. (20) and (21)) [29, 70]. If the applied current density exceeds the optimum amount, a large part of the electricity will be converted into heat energy, increasing the temperature of the wastewater, resulting in increased costs as energy is wasted. These undesirable reactions might be the reason for unchanging dye removal efficiency (from 96.54% to 99.34%) when the current density is raised from 1.33 mA/cm^2 to 1.78 mA/cm^2.

Effect of initial dye concentration on removal efficiency and rate constant

To explain the impact of ARV-3RN dye concentration on the degradation efficiency, various investigations were carried out with ARV-3RN dye concentrations ranging

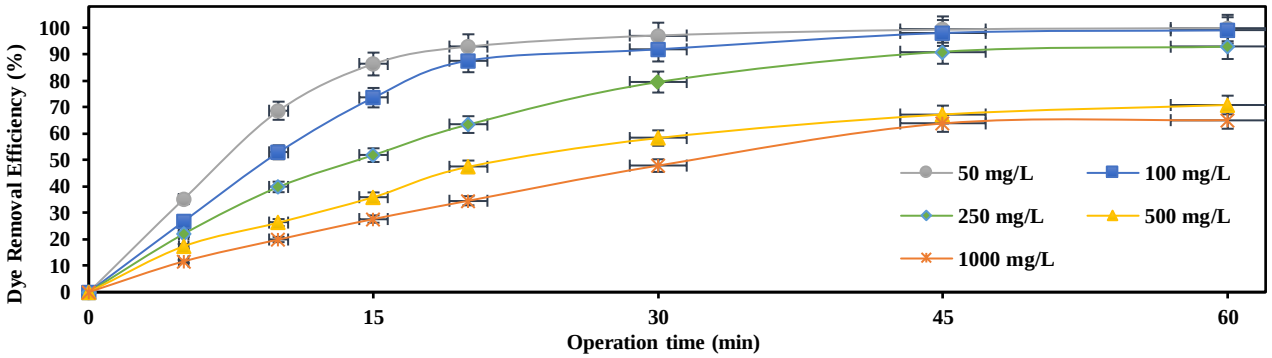

Fig. 11: Effect of initial dye concentration on ARV-3RN dye removal efficiency

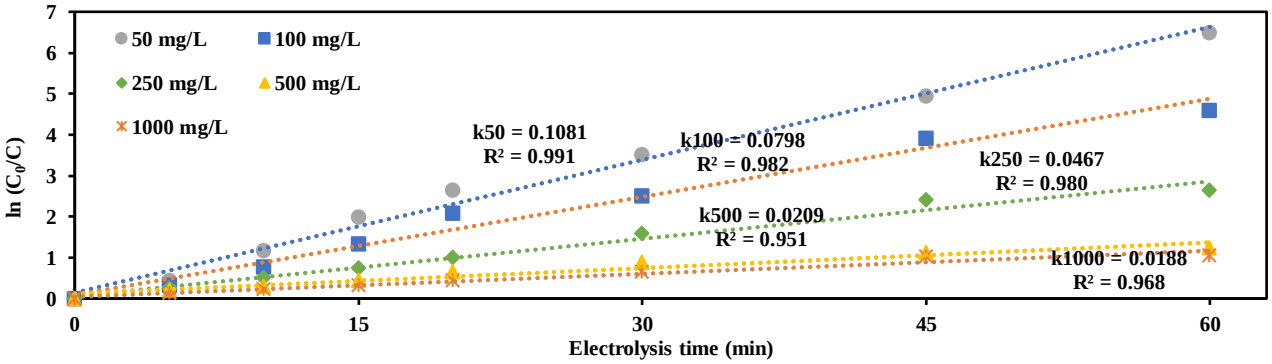

Fig. 12: Pseudo-first-order kinetics fitting for initial dye concentration

from 50 mg/L to 1000 mg/L in the presence of 5.0 mM NaCl, the current density of 0.44 mA/cm^2, initial pH ≈7.5, the temperature of 20 °C, and reaction time of 60 min. As shown in Fig. 11. after 60 min of degradation, the decolorization efficiency of the dye with ARV-3RN dye 50 mg/L and 100 mg/L is 99.84% and 98.99%, while the color removal rates of 250 mg/L, 500 mg/L, and 1000 mg/L were 92.79%, 70.74%, and 65.02%, respectively. Higher degrading efficiency of ARV-3RN dye was obtained for concentrations of 50 mg/L and 100 mg/L. It may be attributed to diffusion control affecting how the dye degrades. As the dye concentration increases, the diffusion rate of the dye molecules to the active sites of the anode decreases, so it tends to form clusters with low diffusion. [35]. Another reason might be that because the amount of •OH and other reactive species generated during electrolysis stayed unchanged at a constant current density, the operated EAOP system in the high concentration of ARV-3RN dye could not remove all of the dye [74].

As seen in Fig. 12. the relationship R^2 = 0.99 is close to 1, and the linear fit between the $\ln C_0/C$ and electrolysis time can be approximated as first-order kinetics. It is observed from Fig. 13 that the rate constant of ARV-3RN oxidation diminished from 0.1081 1/min to 0.0188 1/min when the initial ARV-3RN dye concentration increased from 50 mg/L to 1000 mg/L. This may be because dyes often relate increased initial concentration to clusters of poor diffusivities [56]. The high initial concentration of the ARV-3RN dye might cause generating and accumulation of huge quantities of intermediates and by-products, which compete with the dye molecules to react with the •OH, reducing the removal rate [75, 76]. But at lower concentrations, the maximum ARV-3RN dye removal rate was achieved, indicating that •OH radicals destroyed most of the dye molecules. A process can explain this result in which, at low initial concentrations, the rates of the electrochemical breakdown of organic molecules might be faster than the diffusion of intermediate metabolites [75, 77].

Effect of temperature on removal efficiency and rate constant

As shown in Fig. 13. the effects of different temperatures (10 °C, 20 °C, 30 °C, 40 °C, and 55 °C) on color removal rates were investigated at 0.44 mA/cm^2 current density, 250 mg/L ARV-3RN dye concentration,

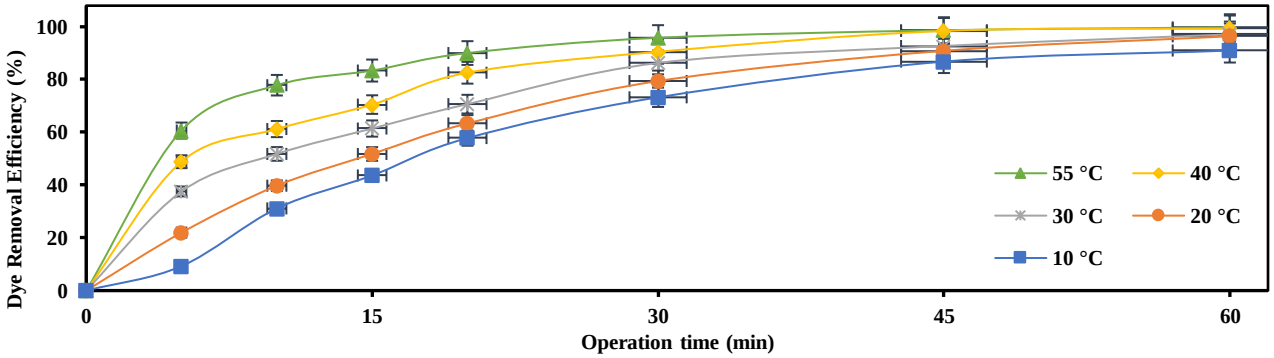

Fig. 13: Effect of temperature on color removal efficiency

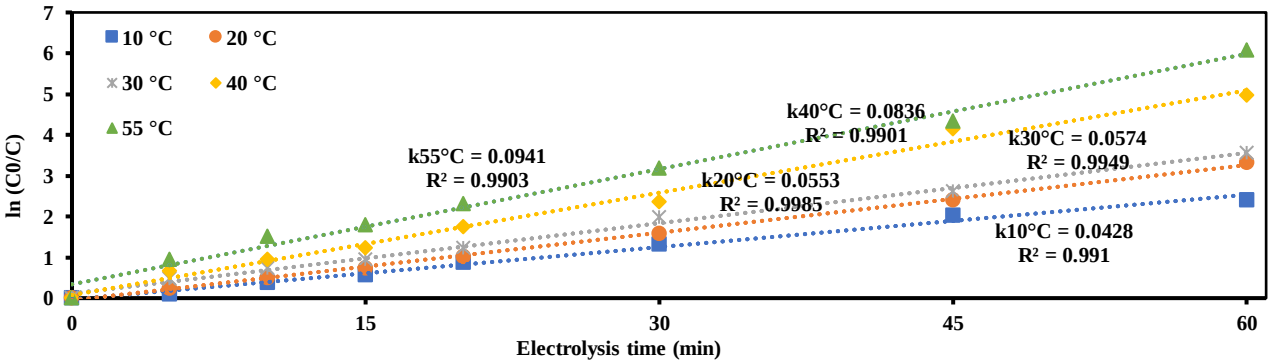

***Fig. 14:** Pseudo-first-order kinetics fitting for temperature*

initial pH (≈7.5), and 60 min operation time. The increasing temperature has a minor effect on the removal efficiency of the ARV-3RN dye. For example, after 60 min of electrochemical degradation, the removal efficiencies at 10 °C, 20 °C, 30 °C, 40 °C, and 55 °C are 90.99%, 96.39%, 97.11%, 99.31%, and 99.77%, respectively. The effect of temperature may vary for each pollutant. While some researchers have found that organic matter oxidises more quickly as the temperature rises, other investigations have shown the converse to be true. The mass transfer process increases as the increasing temperature decreases the solution viscosity [78]. A possible enhancement of removal efficiency of ARV-3RN dye could be attributed to an increase in the pollutant's contact with the electrode and an increase in the pollutant's interaction with oxidising agents (•OH, HClO, and ClO^-) in the solution [58]. Depending on the type of mediated oxidants, the increasing temperature can also increase the rate of mediated oxidation [79–81]. Additionally, when the temperature of the solution rises, the applied voltage drops, which lowers energy usage. The first-order kinetic constants k ranged from 0.0941-0.0428 1/min according to the investigated temperature values. As seen in Fig. 14. the decolourisation efficiency gradually increased at temperatures of 10 °C, 20 °C, and 30 °C, but when the temperature reached 40 °C, and 50 °C, the same change in temperature was near twice the corresponding degradation efficiency. When the temperature rises to 50 °C, the reaction energy barrier is decreased, leading to a dramatic increase of molecules in a high-energy state.

Several steps can be carried out to analyse the regulating mechanism of the electrooxidation, such as chemical reaction, diffusion control, and mass transfer. Kinetic models were used to test experimental results from the oxidation of ARV-3RN dye on $Ti/IrO_2/RuO_2$. The kinetic parameters, which are beneficial for the prediction of oxidation rate, supply important data for designing and modelling the EAOP processes. Thus, the kinetics of electrooxidation of the ARV-3RN dye on $Ti/IrO_2/RuO$ was analyzed using pseudo-zero order, pseudo-first order and pseudo-second order. The results of the kinetic analysis are given in Table 3. It was found that the data were fitted with the pseudo-first-order kinetic model.

Table 3. Kinetic constants for electrooxidation of ARV-3RN dye on Ti/IrO₂/RuO

Parameters						Kinetic Models					
						Pseudo-zero order	Pseudo-second order	Pseudo-first order			
Support electrolyte type	Support electrolyte concentration (mol/L)	Initial dye concentration (mg/L)	pH	Current density (mA/cm²)	Temperature ̊C	R^2	R^2	Experimental C_o	Calculated C_o	k (1/min)	R^2
NaCl	5	250	7.5	0.44	20	0.859	0.945	250	248.2	0.0467	0.984
KCl	5	250	7.5	0.44	20	0.855	0.910	250	247.3	0.0353	0.965
$NaNO_3$	5	250	7.5	0.44	20	0.929	0.916	250	246.1	0.0128	0.959
Na_2SO_4	5	250	7.5	0.44	20	0.880	0.898	250	243.0	0.0076	0.912
Without	0	250	7.5	0.44	20	0.912	0.933	250	245.8	0.0045	0.952
NaCl	2.5	250	7.5	0.44	20	0.930	0.911	250	244.6	0.0239	0.979
NaCl	7.5	250	7.5	0.44	20	0.794	0.926	250	242.3	0.0518	0.986
NaCl	10	250	7.5	0.44	20	0.719	0.745	250	248.7	0.0718	0.991
NaCl	5	50	7.5	0.44	20	0.541	0.691	50	48.31	0.1081	0.991
NaCl	5	100	7.5	0.44	20	0.662	0.854	100	98.55	0.0798	0.982
NaCl	5	500	7.5	0.44	20	0.887	0.918	500	495.0	0.0209	0.951
NaCl	5	1000	7.5	0.44	20	0.936	0.967	1000	989.4	0.0188	0.968
NaCl	5	250	3.0	0.44	20	0.633	0.691	250	251.3	0.0906	0.990
NaCl	5	250	5.0	0.44	20	0.709	0.871	250	254.3	0.0664	0.986
NaCl	5	250	9.0	0.44	20	0.928	0.926	250	246.9	0.0194	0.974
NaCl	5	250	11.0	0.44	20	0.916	0.929	250	240.7	0.0174	0.969
NaCl	5	250	7.5	0.89	20	0.826	0.951	250	244.4	0.0489	0.982
NaCl	5	250	7.5	1.33	20	0.842	0.912	250	244.3	0.0556	0.989
NaCl	5	250	7.5	1.78	20	0.800	0.771	250	252.0	0.0837	0.995
NaCl	5	250	7.5	0.44	10	0.865	0.944	250	251.4	0.0426	0.990
NaCl	5	250	7.5	0.44	30	0.867	0.836	250	252.3	0.0574	0.994
NaCl	5	250	7.5	0.44	40	0.824	0.805	250	251.7	0.0835	0.990
NaCl	5	250	7.5	0.44	55	0.707	0.789	250	248.4	0.0855	0.984

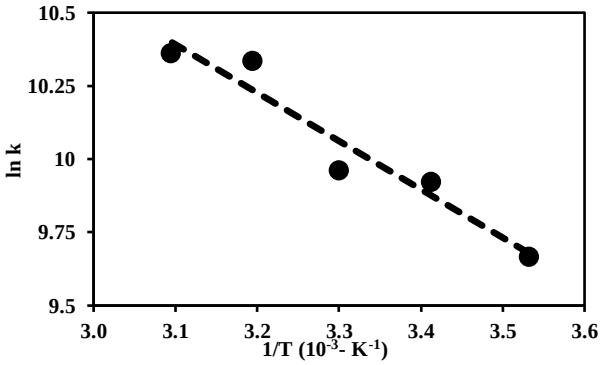

Fig. 15: The Arrhenius plots for electrooxidation of ARV-3RN dye on Ti/IrO₂/RuO₂.

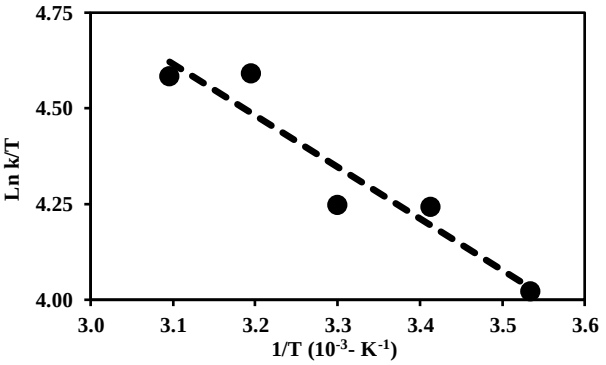

Fig. 16: Eyring plot used to determine ΔH and ΔS

Activation Energy and Thermodynamic Parameters

The Arrhenius equation describes the quantitative relationship between assay temperature, rate constant, and activation energy. The dependence of the oxidation rate constant on temperature can be given as follows [82].

$$Ln(k) = Ln(k_a) - \frac{E_a}{R_g} \cdot \frac{1}{T} \quad (24)$$

where Ea, activation energy (kJ/mol); k_a, Arrhenius constant; Rg, universal gas constant (8.314 J/mol-K); T the absolute temperature (K); k global apparent rate constant (1/min).

According to the Arrhenius equation (Eq. (24)), to calculate k_0 and Ea values for different temperatures can be plotted the graph of ln (k) vs 1/T. Fig. 3a shows the pilot of ln(k) versus 1/T, giving a straight line. In the aqueous solution, activation energy (E_a) was found to be 13.707 kJ/mol for the electrooxidation of the ARV-3RN dye on Ti/IrO₂/RuO.

Thermodynamics Parameters

Thermodynamic activation parameters Gibbs free energy (ΔG), enthalpy (ΔH) and entropy of activation (ΔS) changes were determined using Eyring's equation [83, 84].

$$Ln\left(\frac{k}{T}\right) = \left[Ln\left(\frac{k_b}{h}\right) + \frac{\Delta S*}{R_G}\right] - \frac{\Delta H*}{R_G} \cdot \frac{1}{T} \quad (25)$$

Where k_b and h are the Boltzmann constant (R_g=N, 1.3806x10^{-23} J/mol-K) and Plank's constant (6.60266x 10^{-34} J/s), respectively. T is the absolute temperature (K) and R_G is the universal gas constant (kJ/mol-K).

If we plot an Ln(k/T) versus 1/T, from the intercept is calculated the change in entropy (ΔS), and by the slope, it is possible to calculate the change in enthalpy (ΔH). The Gibbs free energy (ΔG) of a system (ΔG) can be determined from the following equation [85]. The ln (k/T) versus (1/T) is given in Fig. 16.

$$\Delta G* = \Delta H* - T \cdot \Delta S* \quad (26)$$

The formation of complex activated molecules is linked to the activation entropy (ΔS). A negative sign means the number of molecules in the system decreases when the species are combined in the transition state. On the other hand, the system gets more disorganised, and the value of ΔS decreases when more components are present in the transition state. An increase in the number of species and resulting randomness at the (solid + liquid) interface are both clarified by a negative ΔS [33]. The energy used by the reactions that occur during oxidation is known as the enthalpy of activation (ΔH) [86]. Positive ΔH and ΔG values indicate that the reaction is endothermic and nonspontaneous since the product's enthalpy is higher than the reactants, while the endergonic reaction is represented by negative ΔS [87,88]. The values of ΔH, ΔS and ΔG are shown in Table 4.

Energy Consumption

The electrooxidation process's primary drawback is its significant energy consumption. Therefore, the efficiency of electrooxidation processes is generally evaluated regarding energy consumption. The variances in energy consumption for experimental parameters are seen in Fig.17. When the results were evaluated, it became clear that the supporting electrolyte type greatly impacts how much energy is used. High conductivity generally corresponds to reduced electrochemical cell resistance and higher process efficiency. Each support electrolyte type used less energy than running without support electrolytes. Intentionally adding a supporting electrolyte such as NaCl, KCl, $NaNO_3$, and Na_2SO_4 increases the conductivity of synthetic wastewater decreases electrical energy usage and promotes indirect anodic oxidation. As seen in Fig. 17 (a).

Table 4: Thermodynamic parameters for the electrooxidation of the ARV-3RN dye on Ti/IrO₂/RuO

ΔH (kJ/mol)	ΔS (J/mol-K)	ΔG (kJ/mol)				
		293 K	303 K	313 K	323 K	333 K
11.196	-0.1244	47.662	48.907	50.152	51.396	52.641

Depending on the support electrolyte type, the energy consumptions for NaCl, KCl, $NaNO_3$, and Na_2SO_4 were calculated at 3.10 kW-h/m^3, 3.18 kW-h/m^3, 4.79 kW-h/m^3, and 4.94 kW-h/m^3, respectively. Because of an increase in the electrical conductivity of the solution, low energy consumption results from a reduction in the potential difference applied at a constant current [89]. NaCl has the lowest energy requirement compared with other salts due to its high solubility and effective ionisation in solution. When choosing the electrolyte type, it is important to consider the indirect removal efficiency of pollutants, ionisation, the ability to minimise the potential difference, behaviour to reduce energy consumption, and other factors. The electrochemical treatment of wastewater requires high ionic strength to give enough solution conductivity. As seen in Fig. 17 (b). for certain concentrations of 2.5 mM, 5.0 mM, 7.5 mM, and 10 mM NaCl, energy consumption values may be reported as follows: 4.21 kW-h/m^3, 3.10 kW-h/m^3, 2.96 kW-h/m^3, and 2.60 kW-h/m^3, respectively. The electrical conductivity of the solution increased with an increase in electrolyte concentration, and as a result, the electrolytic cell voltage required to maintain a constant current decreased. As seen in Fig. 17 (c). the highest amount of energy used per m^3 of wastewater is as follows: natural pH (≈7.5) > pH 3.0 > pH 9.0 > pH 5.0 > pH 11.00 for initial pH values. Because a high conductivity of the medium is necessary for reduced energy consumption. This is because HNO_3 and NaOH added to the synthetic dye solution at constant current density (0.44 mA/cm^2) increase the wastewater's conductivity, and the conductivity increase reduces the potential difference. The quantity of oxidants (active chlorine and •OH) produced at the anode is controlled by the current density, a crucial variable in the AO process. The two key operational factors affecting process cost are applied current and voltage. The voltage supplied to the system increases as the current density increase, and as the voltage rises, so does energy consumption. As seen in Fig. 17 (d). according to the current densities of 0.44 mA/cm^2, 0.89 mA/cm^2, 1.33 mA/cm^2, and 1.78 mA/cm^2, the effects of which were examined, the energy consumption was calculated at 3.10 kW-h/m^3, 8.183 kW-h/m^3, 16.20 kW-h/m^3, and 25.767 kW-h/m^3, respectively. Consequently, the increase in current density leads to a considerable rise in energy consumption. Since it takes longer for the system to reach equilibrium, oxidation of organic substances in the environment takes longer at low current densities, but there is a decrease in energy use. Energy consumption also rises while the reaction time is sped up at greater current densities. It is crucial to consider both the value with the highest removal rate and the current density with the lowest energy usage when selecting the optimum current density. As seen in Fig. 17 (e). energy consumption based on initial dye concentration was found to be 2.71 kW-h/m^3, 2.83 kW-h/m^3, 3.10 kW-h/m^3, 5.20 kW-h/m^3, and 6.73 kW-h/m^3 for 50 mg/L, 100 mg/L, 250 mg/L, 500 mg/L, and 1000 mg/L in 60 min electrolysis time. The energy consumption in the electrooxidation process tended to increase as the dye concentration decreased. The electrooxidation process with the lowest energy consumption consisted of the one that used a dye concentration of 1000 mg/L. Related to this, it can be explained as the decrease in conductivity of the solution with decreasing dye concentration. The system's resistance increases due to the decreased concentration since it decreases the pollutants in the wastewater per unit volume. The increased system resistance reduces electrical conduction and increases direct and indirect oxidation energy requirements. When Fig. 17 (f). is examined, energy consumption in the run operated at 55 °C was the lowest with 2.50 kW-h/m³. It was obtained as 2.79 kW-h/m³ for 40°C, 2.93 kW-h/m³ for 30°C, 3.10 kW-h/m³ for 20°C and 3.52 kW-h/m³ for 10 ˚C. Because when temperature increases, pollutants are more likely adsorption to the anode surface for direct oxidation, and resistance is reduced. Water becomes more fluid as the temperature rises, and the electric current supplied into the system promotes the production of intermediate agents that promote indirect electrooxidation for the degradation of pollutants is another advantageous consequence.

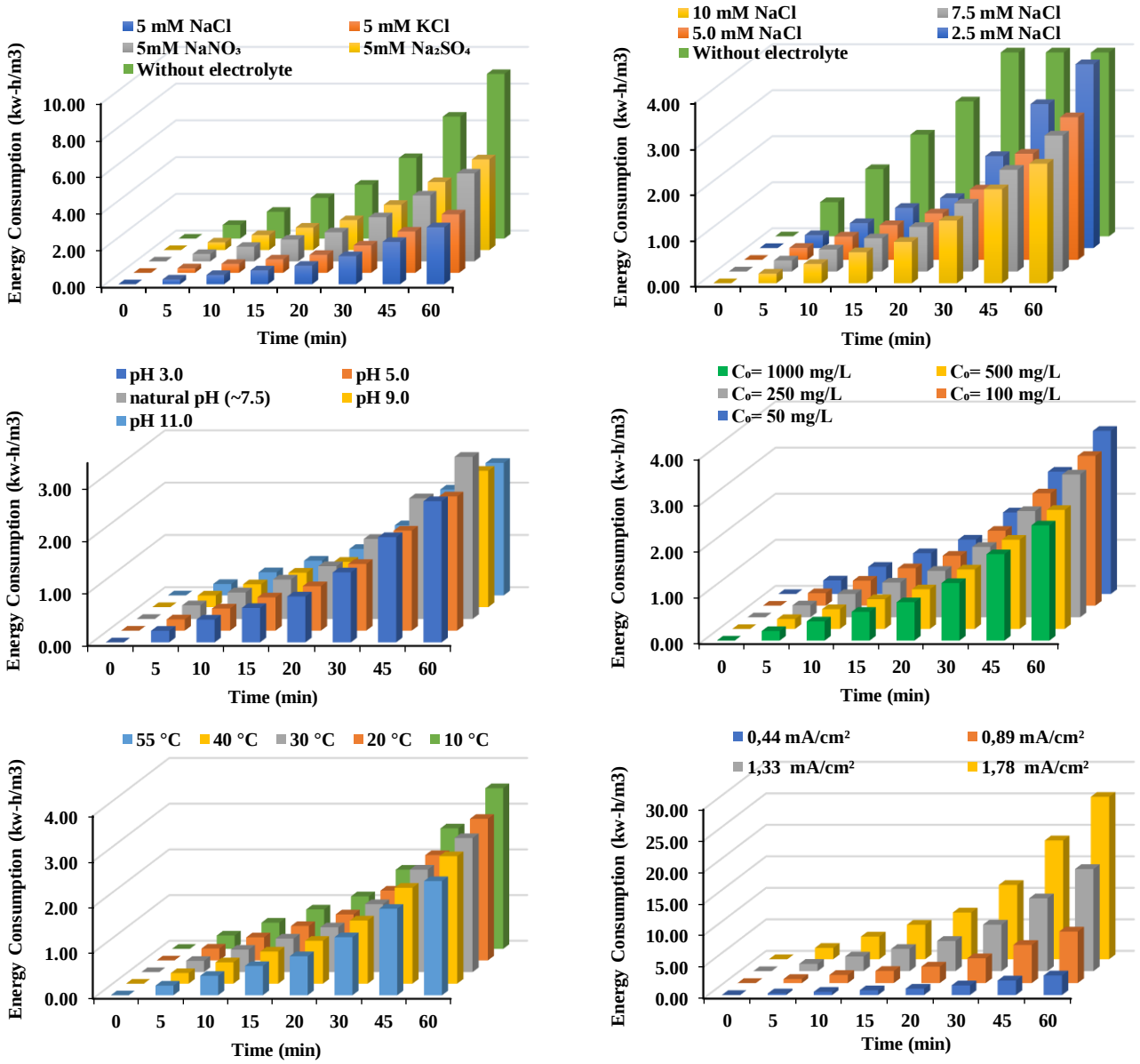

Fig. 17: Energy consumption; (a) Support electrolyte type, (b) Support electrolyte concentration, (c) initial Ph, (d) current density, (e) Dye concentration, (f) temperature

CONCLUSIONS

Electrochemical oxidation is an effective process for dye removal, and high removal efficiencies have been obtained predominantly from indirect oxidation. In summary, better and more affordable technology for degrading organic pollutants can only be possible with excellent knowledge of the variables affecting the electrooxidation process. Firstly, the use of different types of support electrolytes (NaCl, KCl, $NaNO_3$, and Na_2SO_4) was investigated in this study. In terms of dye removal efficiency and energy consumption, the high dye removal efficiency (92.79%) was obtained in the study using NaCl with the least energy consumption (3.10 kW-h/m^3). After determining the supporting electrolyte type, the highest dye removal efficiency was found to be 98.87% in the study with a concentration of 10 mM NaCl. Increasing the amount of supporting electrolytes resulted in a decrease in energy consumption. Although the oxidation of ARV-3RN in an acidic medium (pH=3.0 (99.67%) and (pH=5.0 (98.14%)) and natural pH (≈7.5 (92.79%) was efficient and high, ARV-3RN removal was severely negatively affected by the basic pH values (pH=9.0 (69%) and pH=11 (62.97%)). Significant

degradation of the synthetic dye ranging between 92.79% and 99.34% was accomplished at all current densities (0.44 mA/cm^2, 0.89 mA/cm^2, 1.33 mA/cm^2, and 1.78 mA/cm^2) applied in this study. However, since it is evaluated in terms of energy consumption, increasing the current density from 0.44 mA/cm^2 to 1.78 mA/cm^2 dramatically increased the energy consumption from 3.1kW-h/m^3 to 25.76 kW-h/m^3. Examining how the initial dye concentration affects the electrochemical oxidation process is crucial because industrial effluents often have a varying concentration range. It can be the statement that both the removal efficiency and the rate constant of the ARV-3RN dye were negatively impacted by increasing the initial dye concentration. The temperature increase promotes faster deterioration and less energy consumption because it generally increases the mass transfer process due to decreased solution viscosity with increasing temperature.

Received: Dec. 21, 2022; Accepted: May. 22, 2023

REFERENCES

[1] Jun L.Y., Yon L.S., Mubarak N.M., Bing C.H., Pan S., Danquah M.K., Abdullah E.C., Khalid M., An Overview of İmmobilized Enzyme Technologies for Dye and Phenolic Removal from Wastewater, *J. Environ. Chem. Eng.*, **7:** 102961 (2019).

[2] Ajiboye T.O., Oyewo O.A., Onwudiwe D.C., Simultaneous Removal of Organics and Heavy Metals from İndustrial Wastewater: A Review, Chemosphere, **262:** 128379 (2021).

[3] Bazrafshan E., Mohammadi L., Ansari-Moghaddam A., Mahvi A.H., Heavy Metals Removal from Aqueous Environments by Electrocoagulation Process–A Systematic Review, *J. Environ. Heal. Sci. Eng*., **13:** 74 (2015).

[4] Peramune D., Manatunga D.C., Dassanayake R.S., Premalal V., Liyanage R.N., Gunathilake C., Abidi N., Recent Advances in Biopolymer-based Advanced Oxidation Processes for Dye Removal Applications: A Review, *Environ. Res*., **215:** 114242 (2022).

[5] Tkaczyk A., Mitrowska K., Posyniak A., Synthetic Organic Dyes as Contaminants of the Aquatic Environment and their İmplications for Ecosystems: A Review, *Sci. Total Environ.*, **717:** 137222 (2020).

[6] Lanka S., Gantala S.N., Pandrangi S.L., Chitosan and Chitosan-based Nanocomposite Membranes in the Removal of Synthetic Dye from Effluent Wastewaters, *Text. Waste. Treat.*, 169-177 (2022).

[7] İrdemez Ş., Özyay G., Torun F.E., Kul S., Bingül Z., Comparison of Bomaplex Blue CR-L Removal by Adsorption Using Raw and Activated Pumpkin Seed Shells, *Ecol. Chem. Eng. S.*, **29:** 199-216 (2022).

[8] Gambhir R.S., Kapoor V., Nirola A., Sohi R., Bansal V., Water Pollution: Impact of Pollutants and New Promising Techniques in Purification Process, *J. Hum. Ecol*., **37(2):** 103-109 (2012).

[9] Mella B., Puchana-Rosero M.J., Costa D.E.S., Gutterres M., Utilization of Tannery Solid Waste as an Alternative Biosorbent for Acid Dyes in Wastewater Treatment, *J. Mol. Liq.*, **242:** 137 (2017).

[10] Akbari N., Nabizadeh Chianeh F., Arab A., Efficient Electrochemical Oxidation of Reactive Dye Using a Novel Ti/NanoZnO–CuO Anode: Electrode Characterization, Modeling, and Operational Parameters Optimization, *J. Appl. Electrochem*., **52:** 189-202 (2022).

[11] Sözüdoğru O., Fil B.A., Boncukcuoğlu R., Aladağ E., Kul S., Adsorptive Removal of Cationic (BY2) Dye from Aqueous Solutions onto Turkish Clay: Isotherm, Kinetic, and Thermodynamic Analysis, *Part. Sci. Technol*., **34:** 103-101 (2016).

[12] Okoniewska E., Removal of Selected Dyes on Activated Carbons, *Sustainability*, **13:** 4300 (2021).

[13] Márquez A.A., Coreño O., Nava J.L., A Hybrid Process Combining Electrocoagulation and Active Chlorine-Based Photoelectro-Fenton-Like Methods during the Removal of Acid Blue 29 Dye, *J. Electroanal. Chem.*, **922:** 116732 (2022).

[14] Jayaraman S., Thiruvenkadam V., Experimental and Optimization Studies for the Adsorption of Cationic Dyes from Synthetic Waste Water on the Biomass of Orthophosphoric Acid Activated Barks of Prosopis Cineraria, *Iran. J. Chem. Chem. Eng. (IJCCE)*, **40:** 1067 (2021).

[15] Titchou F.E., Zazou H., Afanga H., El Gaayda J., Ait Akbour R., Lesage G., Rivallin M., Cretin M., Hamdani M., Electrochemical Oxidation Treatment of Direct Red 23 Aqueous Solutions: Influence of the Operating Conditions, *Sep. Sci. Technol*., **57:** 1501 (2022).

[16] Fanaee M., Vahid B., Treatment of Direct Red 23 in Recirculating Semi-Pilot System by O_3/UV Process: Operational Parameters Effect and Central Composite Design Modeling, *Iran. J. Chem. Chem. Eng. (IJCCE)*, **41:** 1755 (2022).

[17] Khataee A.R., Kasiri M.B., Photocatalytic Degradation of Organic Dyes in the Presence of Nanostructured Titanium Dioxide: Influence of the Chemical Structure of Dyes, *J. Mol. Catal. A Chem*., **328:** 8 (2010).

[18] Asadullah M., Asaduzzaman M., Kabir M.S., Mostofa M.G., Miyazawa T., Chemical and Structural Evaluation of Activated Carbon Prepared from Jute Sticks for Brilliant Green Dye Removal from Aqueous Solution, *J. Hazard. Mater*., **174:** 437 (2010).

[19] Tran H.T., Lin C., Bui X.-T., Nguyen M.K., Cao N.D.T., Mukhtar H., Hoang H.G., Varjani S., Ngo H.H., Nghiem L.D., Phthalates in the Environment: Characteristics, Fate and Transport, and Advanced Wastewater Treatment Technologies, *Bioresour. Technol.*, **344:** 126249 (2022).

[20] Kubra K.T., Salman M.S., Hasan M.N., Enhanced Toxic Dye Removal from Wastewater Using Biodegradable Polymeric Natural Adsorbent, *J. Mol. Liq*., **328:** 115468 (2021).

[21] Divyapriya G., Singh S., Martínez-Huitle C.A., Scaria J., Karim A.V, Nidheesh P.V, Treatment of Real Wastewater by Photoelectrochemical Methods: an Overview, *Chemosphere*, **276:** 130188 (2021).

[22] Ameta S., Ameta R., "Advanced Oxidation Processes for Wastewater Treatment: Emerging Green Chemical Technology", Elsevier, London (2018).

[23] Manikandan P., Palanisamy P.N., Baskar R., Sakthisharmila P., Sivakumar P., A Comparative Study on the Competitiveness of Photo-Assisted Chemical Oxidation (PACO) with Electrocoagulation (EC) for the Effective Decolorization of Reactive Blue Dye, *Iran. J. Chem. Chem. Eng. (IJCCE)*, **36:** 71 (2017).

[24] Martínez-Huitle C.A., Panizza M., Electrochemical Oxidation of Organic Pollutants for Wastewater Treatment, *Curr. Opin. Electrochem.*, **11:** 62 (2018).

[25] Ghribi A., Bagane M., Removal of Congo Red and Rhodamine B Dyes from Aqueous Solution by Fenton Process: Optimization of Operational Parameters, *Iran. J. Chem. Chem. Eng. (IJCCE)*, **42(3):** 801-809 (2023).

[26] Shin Y.-U., Yoo H.-Y., Ahn Y.-Y., Kim M.S., Lee K., Yu S., Lee C., Cho K., Kim H., Lee J., Electrochemical Oxidation of Organics in Sulfate Solutions on Boron-Doped Diamond Electrode: Multiple Pathways for Sulfate Radical Generation, *Appl. Catal. B Environ*., **254:** 156 (2019).

[27] Hodges B.C., Cates E.L., Kim J.-H., Challenges and Prospects of Advanced Oxidation Water Treatment Processes Using Catalytic Nanomaterials, *Nat. Nanotechnol.*, **13:** 642 (2018).

[28] Ekrami-Kakhki M.-S., Farzaneh N., Abbasi S., Makiabadi B., Electrocatalytic Activity of Pt Nanoparticles Supported on Novel Functionalized Reduced Graphene Oxide-Chitosan for Methanol Electrooxidation, *J. Mater. Sci. Mater. Electron.*, **28:** 12373 (2017).

[29] Ozturk D., Yilmaz A.E., Treatment of Slaughterhouse Wastewater with the Electrochemical Oxidation Process: Role of Operating Parameters on Treatment Efficiency and Energy Consumption, *J. Water Process Eng.*, **31:** 100834 (2019).

[30] Bassyouni D.G., Hamad H.A., El-Ashtoukhy E.-S.Z., Amin N.K., El-Latif M.M.A., Comparative Performance of Anodic Oxidation and Electrocoagulation as Clean Processes for Electrocatalytic Degradation of Diazo Dye Acid Brown 14 in Aqueous Medium, *J. Hazard. Mater*., **335:** 178 (2017).

[31] Nidheesh P.V, Zhou M., Oturan M.A., An Overview on the Removal of Synthetic Dyes from Water by Electrochemical Advanced Oxidation Processes, *Chemosphere*, **197:** 210 (2018).

[32] Scaria J., Nidheesh P.V., Comparison of Hydroxyl-Radical-based Advanced Oxidation Processes with Sulfate Radical-based Advanced Oxidation Processes, *Curr. Opin. Chem. Eng*., **36:** 100830 (2022).

[33] Naeimi A., Ekrami-Kakhki M.-S., Donyagard F., Enhanced Electrocatalytic Performance of Pt Nanoparticles İmmobilized on Novel Electrospun PVA@Ni/NiO/Cu Complex Bio-Nanofiber/Chitosan based on Calotropis Procera Plant for Methanol Electro-Oxidation, *Int. J. Hydr. Ene.*, **46:** 18949 (2021).

[34] Nidheesh P.V, Zhou M., Oturan M.A., An Overview on the Removal of Synthetic Dyes from Water by Electrochemical Advanced Oxidation Processes, *Chemosphere*, **197:** 210 (2018).

[35] Baddouh A., Rguiti M.M., El Ibrahimi B., Hussain S., Errami M., Tkach V., Bazzi L., Hilali M., Anodic Oxidation of Methylene Blue Dye from Aqueous Solution Using SnO_2 Electrode, *Iran. J. Chem. Chem. Eng. (IJCCE)*, **38:** 175 (2019).

[36] Özyonar F., Korkmaz M.U., Sequential Use of the Electrocoagulation-Electrooxidation Processes for Domestic Wastewater Treatment, *Chemosphere*, **290:** 133172 (2022).

[37] Biswas B., Goel S., Electrocoagulation and Electrooxidation Technologies for Pesticide Removal from Water or Wastewater: A Review, *Chemosphere*, **302:** 134709 (2022).

[38] Fıl B.A., Boncukcuoğlu R., Yilmaz A.E., Bayar S., Electro-Oxidation of Pistachio Processing Industry Wastewater Using Graphite Anode, *Clean–Soil, Air, Water*, **42:** 1232 (2014).

[39] Kul S., Boncukcuoglu R., Yilmaz A.E., Fil B.A., Treatment of Olive Mill Wastewater with Electro-Oxidation Method, *J. Electrochem. Soc.*, **162:** G41 (2015).

[40] Madsen H.T., Søgaard E.G., Muff J., Study of Degradation İntermediates Formed During Electrochemical Oxidation of Pesticide Residue 2, 6-Dichlorobenzamide (BAM) at Boron Doped Diamond (BDD) and Platinum–İridium Anodes, *Chemosphere*, **109:** 84 (2014).

[41] Garcia-Segura S., Ocon J.D., Chong M.N., Electrochemical Oxidation Remediation of Real Wastewater Effluents — A Review, *Process Saf. Environ. Prot.*, **113:** 48 (2018).

[42] Scaria J., Nidheesh P.V., Comparison of Hydroxyl-Radical-Based Advanced Oxidation Processes with Sulfate Radical-based Advanced Oxidation Processes, *Curr. Opin. Chem. Eng.*, **36:** 100830 (2022).

[43] Ekrami-Kakhki M.-S., Farzaneh N., Fathi E., Superior Electrocatalytic Activity of $PtSrCoO_3$−δ Nanoparticles Supported on Functionalized Reduced Graphene Oxide-Chitosan for Ethanol Oxidation, *International Journal of Hydrogen Energy*, **42:** 21131 (2017).

[44] Değermenci G.D., Removal of Reactive azo Dye Using Platinum-Coated Titanium Electrodes with the Electro-Oxidation Process, *Desalin. Water Treat.*, **218:** 436 (2021).

[45] Khezrianjoo S., Revanasiddappa H.D., Evaluation of Kinetics and Energy Consumption of the Electrochemical Oxidation of Acid Red 73 in Aqueous Media, *Toxicol. Environ. Chem.*, **98:** 759 (2016).

[46] Salazar R., Ureta-Zañartu M.S., González-Vargas C., Brito C. do N., Martinez-Huitle C.A., Electrochemical Degradation of İndustrial Textile Dye Disperse Yellow 3: Role of Electrocatalytic Material and Experimental Conditions on the Catalytic Production of Oxidants and Oxidation Pathway, *Chemosphere*, **198:** 21 (2018).

[47] Jardak K., Dirany A., Drogui P., El Khakani M.A., Electrochemical Degradation of Ethylene Glycol in Antifreeze Liquids Using Boron Doped Diamond Anode, *Sep. Purif. Technol.*, **168:** 215 (2016).

[48] Lakshmipathiraj P., Bhaskar Raju G., Sakai Y., Takuma Y., Yamasaki A., Kato S., Kojima T., Studies on Electrochemical Detoxification of Trichloroethene (TCE) on Ti/IrO_2–Ta_2O_5 Electrode from Aqueous Solution, *Chem. Eng. J.*, **198**–**199:** 211 (2012).

[49] Liu S., Xu L., Huang X., Xie J., Chai Z., Chen X., Electrochemical Dissolution Behavior of Haynes 214 Honeycomb Structure in $NaNO_3$ Solutions for Low Current Density Electrochemical Machining, *J. Mater. Eng. Perform.*, **31:** 3559 (2022).

[50] Wang Y., Kong G., Che C., Zhu Y., Effect of NO_3^- Ion on the Corrosion Behavior of Galvanized Coating in Alkaline Solution, *Corrosion*, **74:** 1421 (2018).

[51] Ekrami-Kakhki M.-S., Pouyamanesh S., Abbasi S., Heidari G., Beitollahi H., Enhanced Electrocatalytic Performance of Pt Nanoparticles Incorporated CeO_2 Nanorods on Polyaniline-Chitosan Support for Methanol Electrooxidation (Experimental and Statistical Analysis), *J. Clust. Sci.*, **32:** 363 (2021).

[52] Panizza M., Cerisola G., Removal of Colour and COD from Wastewater Containing Acid Blue 22 by Electrochemical Oxidation, *J. Hazard. Mater.*, **153:** 83 (2008).

[53] Lakshmipathiraj P., Bhaskar Raju G., Sakai Y., Takuma Y., Yamasaki A., Kato S., Kojima T., Studies on Electrochemical Detoxification of Trichloroethene (TCE) on Ti/IrO_2–Ta_2O_5 Electrode from Aqueous Solution, *Chem. Eng. J.*, **198**–**199:** 211 (2012).

[54] Jojoa-Sierra S.D., Silva-Agredo J., Herrera-Calderon E., Torres-Palma R.A., Elimination of the Antibiotic Norfloxacin in Municipal Wastewater, Urine and Seawater by Electrochemical Oxidation on IrO_2 Anodes, *Science of the Total Environment*, **575:** 1228 (2017).

[55] Sridhar R., Sivakumar V., Prakash Maran J., Thirugnanasambandham K., Influence of Operating Parameters on Treatment of Egg Processing Effluent by Electrocoagulation Process, *Int. J. Environ. Sci. Technol.*, **11:** 1619 (2014).

[56] El-Ashtoukhy E.S.Z., Amin N.K., Abd El-Latif M.M., Bassyouni D.G., Hamad H.A., New İnsights into the Anodic Oxidation and Electrocoagulation Using a Self-Gas Stirred Reactor: A Comparative Study for Synthetic CI Reactive Violet 2 Wastewater, *J. Clean. Prod.*, **167:** 432 (2017).

[57] Yin Q., Wu G., Advances in Direct İnterspecies Electron Transfer and Conductive Materials, Electron Flux, Organic Degradation and Microbial İnteraction, *Biotechnol. Adv.*, **37:** 107443 (2019).

[58] Fil B.A., Günaslan S., Electrooxidation Treatment of Slaughterhouse Wastewater: İnvestigation of Efficiency of Ti/Pt Anode, *Part. Sci. Technol.*, **41(4):** 496-505 (2022).

[59] Baddouh A., Bessegato G.G., Rguiti M.M., El Ibrahimi B., Bazzi L., Hilali M., Zanoni M.V.B., Electrochemical Decolorization of Rhodamine B Dye: Influence of Anode Material, Chloride Concentration and Current Density, *J. Environ. Chem. Eng.*, **6:** 2041 (2018).

[60] Belal R.M., Zayed M.A., El-Sherif R.M., Abdel Ghany N.A., Advanced Electrochemical Degradation of basic Yellow 28 Textile Dye Using IrO_2/Ti Meshed Electrode in Different Supporting Electrolytes, *J. Electroanal. Chem.*, **882:** 114979 (2021).

[61] Fil B.A., Günaslan S., Treatment of Slaughterhouse Wastewaters with Ti/IrO_2/RuO_2 Anode and Investigation of Energy Consumption, *Arab. J. Sci. Eng.*, **48:** 457 (2023).

[62] Malpass G.R.P., Miwa D.W., Mortari D.A., Machado S.A.S., Motheo A.J., Decolorisation of Real Textile Waste Using Electrochemical Techniques: Effect of the Chloride Concentration, *Water Res.*, **41:** 2969 (2007).

[63] Miwa D.W., Malpass G.R.P., Machado S.A.S., Motheo A.J., Electrochemical Degradation of Carbaryl on Oxide Electrodes, *Water Res.*, **40:** 3281 (2006).

[64] Viana D.F., Salazar-Banda G.R., Leite M.S., Electrochemical Degradation of Reactive Black 5 with Surface Response and Artificial Neural Networks Optimization Models, *Sep. Sci. Technol.*, **53:** 2647 (2018).

[65] Piya-areetham P., Shenchunthichai K., Hunsom M., Application of Electrooxidation Process for Treating Concentrated Wastewater from Distillery İndustry with a Voluminous Electrode, *Water Res.*, **40:** 2857 (2006).

[66] Singh S., Lo S.L., Srivastava V.C., Hiwarkar A.D., Comparative Study of Electrochemical Oxidation for Dye Degradation: Parametric Optimization and Mechanism İdentification, *Journal of Environmental Chemical Engineering*, **4:** 2911 (2016).

[67] Rodríguez F.A., Mateo M.N., Aceves J.M., Rivero E.P., González I., Electrochemical Oxidation of Bio-Refractory Dye in a Simulated Textile İndustry Effluent Using DSA Electrodes in a Filter-Press Type FM01-LC Reactor, *Environ. Technol.*, **34:** 573 (2013).

[68] Iskurt C., Keyikoglu R., Kobya M., Khataee A., Treatment of Coking Wastewater by Aeration Assisted Electrochemical Oxidation Process at Controlled and Uncontrolled İnitial pH Conditions, *Separation and Purification Technology*, **248:** 117043 (2020).

[69] Prasad R.K., Srivastava S.N., Electrochemical Degradation of Distillery Spent Wash Using Catalytic Anode: Factorial Design of Experiments, *Chem. Eng. J.*, **146:** 22 (2009).

[70] Maljaei A., Arami M., Mahmoodi N.M., Decolorization and Aromatic Ring Degradation of Colored Textile Wastewater Using İndirect Electrochemical Oxidation Method, *Desalination*, **249:** 1074 (2009).

[71] Xia Y., Wang G., Guo L., Dai Q., Ma X., Electrochemical Oxidation of Acid Orange 7 Azo Dye Using a PbO_2 Electrode: Parameter Optimization, Reaction Mechanism and Toxicity Evaluation, *Chemosphere*, **241:** 125010 (2020).

[72] Rahmani A.R., Godini K., Nematollahi D., Azarian G., Electrochemical Oxidation of Activated Sludge by Using Direct and İndirect Anodic Oxidation, *Desalin. Water Treat.*, **56:** 2234 (2015).

[73] Asaithambi P., Govindarajan R., Yesuf M.B., Alemayehu E., Removal of Color, COD and Determination of Power Consumption from Landfill Leachate Wastewater Using an Electrochemical Advanced Oxidation Processes, *Sep. Purif. Technol.*, **233:** 115935 (2020).

[74] He W., Liu Y., Ye J., Wang G., Electrochemical Degradation of Azo Dye Methyl Orange by Anodic Oxidation on Ti_4O_7 Electrodes, *J. Mater. Sci. Mater. Electron.*, **29:** 14065 (2018).

[75] Wang G., Liu Y., Ye J., Lin Z., Yang X., Electrochemical Oxidation of Methyl Orange by a Magnéli Phase Ti_4O_7 Anode, *Chemosphere*, **241:** 125084 (2020).

[76] Kumar D., Gupta S.K., Electrochemical Oxidation of Direct Blue 86 Dye Using MMO Coated Ti Anode: Modelling, Kinetics and Degradation Pathway, *Chem. Eng. Process. - Process Intensif.*, **181:** 109127 (2022).

[77] Jiani L., Zhicheng X., Hao X., Dan Q., Zhengwei L., Wei Y., Yu W., Pulsed Electrochemical Oxidation of Acid Red G and Crystal Violet by PbO_2 Anode, *J. Environ. Chem. Eng.*, **8:** 103773 (2020).

[78] Liu H., Vecitis C.D., Reactive Transport Mechanism for Organic Oxidation during Electrochemical Filtration: Mass-Transfer, Physical Adsorption, and Electron-Transfer, *J. Phys. Chem. C*, **116:** 374 (2012).

[79] Brillas E., Sires I., Arias C., Cabot P.L., Centellas F., Rodriguez R.M., Garrido J.A., Mineralization of Paracetamol in Aqueous Medium by Anodic Oxidation with a Boron-Doped Diamond Electrode, *Chemosphere*, **58:** 399 (2005).

[80] Panizza M., Barbucci A., Ricotti R., Cerisola G., Electrochemical Degradation of Methylene Blue, *Sep. Purif. Technol.*, **54:** 382 (2007).

[81] Jiang Y., Zhao H., Liang J., Yue L., Li T., Luo Y., Liu Q., Lu S., Asiri A.M., Gong Z., Sun X., Anodic Oxidation for the Degradation of Organic Pollutants: Anode Materials, Operating Conditions and Mechanisms. A Mini Review, *Electrochem. commun.*, **123:** 106912 (2021).

[82] Aladağ E., Fil B.A.A., Boncukcuoğlu R., Sözüdoğru O., Yilmaz A.E.E., Adsorption of Methyl Violet Dye a Textile Industry Effluent onto Montmorillonite-Batch Study, *J. Dispers. Sci. Technol.*, **35(12):** 1737-1744 (2014).

[83] Dougherty R.J., Singh J., Krishnan V. V, Kinetics and Thermodynamics of Oxidation Mediated Reaction in l-Cysteine and its Methyl and Ethyl Esters in Dimethyl Sulfoxide-d6 by NMR Spectroscopy, *J. Mol. Struct.*, **1131:** 196 (2017).

[84] Galvan D., Orives J.R., Coppo R.L., Silva E.T., Angilelli K.G., Borsato D., Determination of the Kinetics and Thermodynamics Parameters of Biodiesel Oxidation Reaction Obtained from an Optimized Mixture of Vegetable Oil and Animal Fat, *Energy & Fuels*, **27:** 6866 (2013).

[85] Kamranifar M., Naghizadeh A., Montmorillonite Nanoparticles in Removal of Textile Dyes from Aqueous Solutions: Study of Kinetics and Thermodynamics, *Iran. J. Chem. Chem. Eng. (IJCCE)*, **36(6):** 127-137 (2017).

[86] Spacino K.R., Borsato D., Buosi G.M., Chendynski L.T., Determination of Kinetic and Thermodynamic Parameters of the B100 Biodiesel Oxidation Process in Mixtures with Natural Antioxidants, *Fuel Process. Technol.*, **137:** 366 (2015).

[87] Oguz E., Equilibrium İsotherms and Kinetics Studies for the Sorption of Fluoride on Light Weight Concrete Materials, *Colloids Surfaces A Physicochem. Eng. Asp.*, **295:** 258 (2007).

[88] Lal K., Garg A., Utilization of Dissolved İron as Catalyst during Fenton-Like Oxidation of Pretreated Pulping Effluent, *Process Saf. Environ. Prot.*, **111:** 766 (2017).

[89] Candia-Onfray C., Espinoza N., Sabino da Silva E.B., Toledo-Neira C., Espinoza L.C., Santander R., García V., Salazar R., Treatment of Winery Wastewater by Anodic Oxidation Using BDD Electrode, *Chemosphere*, **206:** 709 (2018).